



Originally published as:

Taran, M. N., Koch-Müller, M. (2013): FTIR spectroscopic study of natural andalusite showing electronic Fe-Ti charge-transfer processes: zoning and thermal evolution of OH-vibration bands. - *Physics and Chemistry of Minerals*, 40, 1, 63-71

DOI: [10.1007/s00269-012-0547-3](https://doi.org/10.1007/s00269-012-0547-3)

FTIR spectroscopic study of natural andalusite showing electronic Fe-Ti charge-transfer processes: zoning and thermal evolution of OH-vibration bands

Michail N. Taran¹, Monika Koch-Müller²

¹Institute of Geochemistry, Mineralogy and Ore Formation, National Academy of Science of Ukraine, Palladin Ave., 34, 03680 Kyiv-142, Ukraine,

E-mail: m_taran@hotmail.com

² Helmholtz Centre Potsdam, GFZ German Research Centre for Geosciences, Section 3.3, Telegrafenberg, D 327

D-14473 Potsdam, Germany

E-mail: Monika.Koch-mueller@gfz-potsdam.de

Abstract

We investigated a natural Brazilian Fe-Ti-containing andalusite and its thermal behavior by polarized infrared and optical spectroscopy. Polarized infrared spectra of the Brazilian andalusite and their evolution at thermal annealing in air clearly evidence that there are several types of OH-groups in the structure. Optical spectra and their evolution with temperature indicate that the incorporated iron (about 0.43 wt % calculated as FeO) is in the ferrous and ferric state. Incorporation of ferrous iron in the Al-sites of andalusite is discussed as a possible incorporation mechanism for hydrogen. The weakening and disappearance of the $\text{Fe}^{2+}/\text{Ti}^{4+}$ IVCT band in the andalusite spectra under annealing in air is caused by oxidization of Fe^{2+} to Fe^{3+} in IVCT $\text{Fe}^{2+}/\text{Ti}^{4+}$ pairs. The process of oxidation is accompanied by a rearrangement of the hydroxyl groups and dehydration of the sample, especially vivid at the final stage of the thermal annealing at 1200 °C. During thermal annealing structural hydroxyls of different types apparently transform to each other: the most distinct are the hydroxyls causing the doublet at 3516 cm^{-1} and 3527 cm^{-1} (i. e. H bonded to O1) which seem to transform into the hydroxyls causing the line at 3461 cm^{-1} (i.e. H bonded to O2). The infrared spectra scanned across differently colored zones of the crystal clearly show that some amount of hydroxyls is related to $\text{Fe}^{2+}/\text{Ti}^{4+}$ IVCT pairs which are the cause of the red to black coloration of the sample in $\mathbf{E}||\mathbf{c}$ -polarized illumination: it is evident that in a part of the hydroxyl groups OH-vector changes orientation aligning directly along crystallographic \mathbf{a} -axis due to some kind of interaction with $\text{Fe}^{2+}/\text{Ti}^{4+}$ IVCT pairs.

Key words: andalusite, FTIR absorption spectra, OH-groups, thermal behavior

Introduction

Electronic intervalence charge-transfer transition (IVCT) of $\text{Fe}^{2+}/\text{Ti}^{4+}$ type causes the intense coloration and distinct pleochroism of natural Fe, Ti-containing andalusite (e.g. Smith 1977; Smith, Strens 1976). The corresponding broad and intense absorption band can be observed at 20500 cm^{-1} . Lately, we reported that under thermal annealing at oxidizing conditions in air the band evidently displays different thermal stability in darkly and lightly colored zones of andalusite crystals, which differ by Fe and Ti concentrations and, as a result, by the intensity of the $\text{Fe}^{2+}/\text{Ti}^{4+}$ IVCT band itself (Taran and Koch-Müller 2010). We also showed that the weakening and disappearance of the $\text{Fe}^{2+}/\text{Ti}^{4+}$ IVCT band in spectra of andalusite annealed in air at temperatures $\geq 700 \text{ }^\circ\text{C}$ is caused by oxidation of Fe^{2+} belonging to the IVCT $\text{Fe}^{2+}/\text{Ti}^{4+}$ -pairs to Fe^{3+} . A vivid difference in the thermal stability of the IVCT band in lightly- and darkly-colored zones evidences of a self-stabilization of the pairs over some interaction between them, although the mechanism of the interaction is not quite clear.

The absolute concentrations of OH in the three Al_2SiO_5 polymorphs, kyanite, sillimanite, and andalusite, are low compared to many other nominally anhydrous minerals (Johnson 2006). So far, among the three polymorphs the largest OH-content, up to 270 wt. ppm H_2O , was found in an andalusite crystal from an unspecified location in Minas Gerais, Brazil (Rossman 1996; Johnson 2006). While Burt et al. (2007) determined in an analysis of the theoretical electron density distribution in conjunction with IR spectroscopy the oxygens O1 and O2 as potential protonation sites in andalusite, the explicit incorporation mechanism is poorly understood. According to Johnson (2006), hydrogen incorporates via the exchange mechanism $3 \cdot \text{OH}^- + \text{vacancy} \leftrightarrow \text{Al}^{3+} + 3\text{O}^{2-}$, however this is suggested without any proof. Other mechanisms for H incorporation into andalusite are discussed, e.g. substitution of Al^{3+} by two-valent cations such as Fe^{2+} or hydrogarnet substitution (Beran and Zemann 1969; Burt et al. 2007). So far, no

relation has been established between OH-groups and iron or other impurity ions such as Ti in andalusite.

The item of this investigation is to elucidate whether there is any correlation between OH and Fe and Ti ions involved in $\text{Fe}^{2+}/\text{Ti}^{4+}$ IVCT processes in the andalusite structure. Based on the results of the optical spectroscopic study in respect to the $\text{Fe}^{2+}/\text{Ti}^{4+}$ IVCT band in differently colored zones of Fe, Ti-containing andalusites (Taran and Koch-Müller 2010), we carried out FTIR spectroscopic investigations of OH-vibration bands in zoned natural and thermally treated andalusite crystals.

Experimental details

Preliminary FTIR-spectroscopic measurements were carried out on the relatively thin andalusite samples, which were used earlier for optical absorption spectroscopic studies (Taran and Koch-Müller 2010). The measurement were done at ambient conditions on the untreated natural samples and on the same samples but annealed in oxidizing and reducing conditions. We found the most prominent effect on the coloration and the intensity of the $\text{Fe}^{2+}/\text{Ti}^{4+}$ IVCT absorption band in the samples annealed at oxidizing conditions in air. For the OH bands the strongest changes were also revealed under annealing in air. In this study the thermal behavior of the OH-groups was investigated in more detail by polarized FTIR spectroscopy in the range of $4000\text{-}2500\text{ cm}^{-1}$ on a thicker sample, ca. 2.3 mm thick along the **a**- and 3.5 mm along the **b**-axis, through annealing in air. The sample was prepared by grinding and polishing a natural gem quality crystal taken from the same collection of andalusite crystals as those studied lately by Taran and Koch-Müller (2010). The sample was oriented by morphology using well developed crystal faces. The orientation was controlled by conoscopic observation in a polarizing microscope. Visually, with unpolarized light and, more prominent with **E**||**c**-polarized transmitting illumination the sample showed a distinct zoning: its color, caused by electronic

Fe²⁺/Ti⁴⁺ IVCT processes (Smith 1977; Smith and Strens 1976; Taran and Koch-Müller 2010), varied from red (light zones) to brownish-black, almost opaque (dark zones).

Infrared spectra were recorded on a Bruker Vertex 80v FTIR spectrometer, equipped with a Globar light source, a KBr beam-splitter and a Hyperion microscope using Cassegrainian objectives and an InSb detector. The spectra were taken with an aperture size of 50×50 μm and a resolution of 2 cm⁻¹. For each measurement the spectrum was averaged over 256 scans. The spectra are normalized to 1.0 cm thickness. To evaluate energy, peak intensity and half-widths of the bands the Peakfit 4.0 (Jandel Scientific) software was used to fit the spectra with Lorentzian curves after a straight line background correction.

To confirm the nature of the coloration, **E**||**c**-polarized absorption spectra of the two differently colored zones, light and dark (Fig. 1), were measured on the thick sample identical to the procedure described by Taran and Koch-Müller (2010) (see Experimental section).

After the annealing processes and spectra collection, the thick sample was sealed by arc welding in a 50 mm long gold capsule with 4 mm diameter together with 50 μl H₂O. The capsule was placed into a cold seal autoclave and pressurized by water. The sample was first pressurized to 0.5 kbar and then isobarically heated to 650 °C within ~20 minutes. The *f*_{O₂} was close to the nickel-nickeloxide (NNO) buffer by the Ni-bearing material of the autoclave and filler rods. Run duration was 24 hours. The sample was isobarically cooled to ambient temperature in less than five minutes.

Results

Within the uncertainty of the microprobe analyses the composition of the thicker sample is practically the same as the thinner studied before, i.e. (in wt. %), Al₂O₃ = 61.29, SiO₂ = 38.14, with admixture of iron calculated as FeO ≈ 0.43 and traces of titanium. As seen from the Figure 1, the **E**||**c**-polarized optical absorption spectrum of the light zone contains a broad intense Fe²⁺/Ti⁴⁺ IVCT absorption band (cf. Smith 1977; Smith and Strens 1976; Taran and Koch-Müller 2010) which is - due to the sample thickness - too intense and out of scale in the range of 18000

to 23000 cm^{-1} (around the maximum of the $\text{Fe}^{2+}/\text{Ti}^{4+}$ IVCT band). As expected, the band is far more intense in the dark zone and can only be measured as an absorption edge (the low-energy wing of the $\text{Fe}^{2+}/\text{Ti}^{4+}$ IVCT band) which causes a very dense dark-brown, nearly black color of the sample in $\mathbf{E}\|\mathbf{c}$ -polarization. A distinct absorption shoulder feature at around 12000 cm^{-1} superimposed on the edge was assigned to electronic spin-allowed dd -transition ${}^5T_{2g}\rightarrow{}^5E_g$ of ${}^{\text{VI}}\text{Fe}^{2+}$ (Taran and Koch-Müller 2010). In the two other polarizations, $\mathbf{E}\|\mathbf{a}$ and $\mathbf{E}\|\mathbf{b}$, the sample has practically homogeneous light greenish-yellow colors and does not show any definite zoning. Note, that the $\mathbf{E}\|\mathbf{a}$ - and $\mathbf{E}\|\mathbf{b}$ -polarized spectra (not shown) are practically identical to those published by Taran and Koch-Müller (2010).

Polarized FTIR spectra of the two differently colored zones, light and dark, are shown in Fig. 2, **a** and **b**, respectively. As seen, in the range $3200\text{-}3800\text{ cm}^{-1}$ a series of sharp absorption lines $\mathbf{E}\|\mathbf{b} \geq \mathbf{E}\|\mathbf{a} \gg \mathbf{E}\|\mathbf{c}$ exist attributed by Burt et al. (2007) to OH stretching vibrations. We observe sharp absorption lines with similar intensity ratios and polarization behavior in light zones at (in cm^{-1}) 3247, 3275, 3437, 3461, 3480, 3516, 3527, 3598 and 3654, strong in $\mathbf{E}\|\mathbf{a}$ - and $\mathbf{E}\|\mathbf{b}$ -polarizations, but very weak in $\mathbf{E}\|\mathbf{c}$ ¹. The spectra measured in the dark zones show distinct differences in respect to the bands at 3480, 3437, 3598, 3247 and 3275 cm^{-1} : first of all, in the light zones the relatively intense sharp line at 3437 cm^{-1} and a weaker one at 3480 cm^{-1} can be observed in both $\mathbf{E}\|\mathbf{a}$ - and $\mathbf{E}\|\mathbf{b}$ -polarizations with similar intensities, whereas in spectra taken in the dark zones they are present in $\mathbf{E}\|\mathbf{a}$ -polarization but completely absent in $\mathbf{E}\|\mathbf{b}$. Besides, the $\mathbf{E}\|\mathbf{b}$ -polarized line at 3598 cm^{-1} is much weaker in the dark than in the light zone, thus showing a possible relation to the above mentioned lines at 3480 cm^{-1} and 3437 cm^{-1} . On the other hand, a weak doublet of two relatively broad bands at 3247 cm^{-1} and 3275 cm^{-1} ($\mathbf{E}\|\mathbf{b} \approx \mathbf{E}\|\mathbf{a} \gg \mathbf{E}\|\mathbf{c}$) has higher intensity in the dark than in the light zone. Most of these observations are apparent in Figure 3 where a 20 steps straight line scan of $\mathbf{E}\|\mathbf{b}$ -polarized spectra across differently colored

¹ In Burt et al. (2007) the lines in $\mathbf{E}\|\mathbf{c}$ -polarization are even much weaker, practically zero, that may be due to slightly different qualities of the IR polarizers used there and in the present study (see e.g. Libowitzky and Rossmann 1996).

zones of the sample is shown. Particularly, the distinct reverse correlation of the intensity of the absorption line at 3437 cm^{-1} with the density of the red-to-black color (caused by variation in intensity of the $\text{Fe}^{2+}/\text{Ti}^{4+}$ IVCT band at 20500 cm^{-1} , cf. Taran and Koch-Müller 2010) is well traced out. Scanning across the **ac**-plane of the sample reveals that in **E||a**-polarization the two most characteristic lines at 3437 cm^{-1} and 3480 cm^{-1} behave in a similar way. Though, they only considerably weaken in the dark zones, but do not completely disappear as in the **E||b**-polarized spectra in Fig. 3.

On the whole, the integrated absorbance in the spectral range of 3800 cm^{-1} - 3200 cm^{-1} is somewhat higher in the light zone than in the dark one. For comparison we used the calibration proposed by Burt et al. (2007) to quantify water in andalusite (in ppm by weight) as ~ 95 (light) and ~ 76 (dark). These values are close to the values given in Burt et al (2007) ranging from 110 to 170 ppm by weight but much less than the maximum of 270 ppm, reported so far for andalusite by Rossman (1996). The reason for such a difference could be the use of a non-mineral specific absorption coefficient for andalusite (Koch-Müller and Rhede, 2010): Burt et al. (2007) used the kyanite calibration of Bell et al. (2004) to quantify water in andalusite, while Rossman et al. (1996) used IR independent methods.

In this study we focus on the evolution of the OH bands with increasing temperature. On the whole, the thermal evolution of the OH band in both light and dark zones in the temperature range $800 - 1000^\circ\text{C}$ may be described as follows: with increasing temperature the intensities of the split doublet at 3527 cm^{-1} , 3516 cm^{-1} and, in a somewhat lesser extent, of the line 3437 cm^{-1} continually decrease whilst that of the line at 3461 cm^{-1} significantly increases in all three polarizations, **E||a**, **E||b** and **E||c**, probably, at the expense of the former three bands. Under annealing at 1100°C during 2 hours these processes facilitate, especially, the doublet at 3527 cm^{-1} and 3516 cm^{-1} drastically decreased and the line at 3461 cm^{-1} dominates the spectra. However, further heating at 1100°C and, subsequently, at 1200°C leads to a continual decrease of all absorption lines. At these temperatures even the most thermally stable absorption lines at

3598 cm^{-1} and 3654 cm^{-1} , which well kept their intensity at lower temperatures, decrease and bleach out nearly completely. Again, the more intense $\mathbf{E}\parallel\mathbf{a}$ -polarized line at 3654 cm^{-1} is obviously less thermally stable than the weaker line at 3598 cm^{-1} ($\mathbf{E}\parallel\mathbf{a} > \mathbf{E}\parallel\mathbf{b} \gg \mathbf{E}\parallel\mathbf{c}$) (Fig. 5) that inevitably points to the fact that they are caused by OH-groups of different type, apparently having OH-vectors differently oriented within the plane (001). All the above mentioned observations can well be seen from the $\mathbf{E}\parallel\mathbf{b}$ - and $\mathbf{E}\parallel\mathbf{a}$ -spectra of the light zone measured before and after thermal annealing at different temperatures and durations, shown in Fig. 4 and 5, respectively. Polarized infrared spectra of the two zones, light and dark, after annealing at 1100 $^{\circ}\text{C}$ during 10 hours are shown in Fig. 6. We estimate the hydroxyl group content as 61 ppm and 52 ppm of water in the light and the dark zone, respectively, which is noticeably lower than in the initial state (see above). Note, that the line at 3437 cm^{-1} , though significantly decreased, still has a distinct $\mathbf{E}\parallel\mathbf{b}$ -polarized component in the light zone and none in the dark one. Annealing at 1200 $^{\circ}\text{C}$ during five hours induced further drastic changes of the spectra. As seen from Fig. 7, the spectra maintain predominantly one relatively broad absorption line at 3461 cm^{-1} . Note that in the dark zone after annealing at 1100 $^{\circ}\text{C}$ and, especially, at 1200 $^{\circ}\text{C}$ it acquires higher intensity in $\mathbf{E}\parallel\mathbf{a}$ - than in $\mathbf{E}\parallel\mathbf{b}$ -polarization, opposite to what was observed in the initial sample (cf. Figs. 2, 6 and 7). Still, as in the original non-annealed crystal, the characteristic feature of the spectrum of the dark zones is zero intensity of the line at 3437 cm^{-1} in the $\mathbf{E}\parallel\mathbf{b}$ -polarization. It should also be noted that the absorption lines become noticeably broader after thermal treatment. For instance, FWHM (full width at half-maximum) of the $\mathbf{E}\parallel\mathbf{b}$ -polarized line at 3461 cm^{-1} , which maintains in the spectra (Fig. 7), is 12 cm^{-1} in the initial crystal and 14 cm^{-1} after final treatment at 1200 $^{\circ}\text{C}$ during 5 hours.

In contrast to the experiments by Taran and Koch-Müller (2010) (sample thickness 0.488 mm), annealing the sample of this study (thickness > 2 mm) in air at each hundred degrees in the interval 500 $^{\circ}\text{C}$ - 1000 $^{\circ}\text{C}$ for 2 hours induces practically no changes in color. Since the compositions of the two samples are nearly identical and the nature of the coloration and zoning

is the same, we imply that the differences in the thermal behavior of the color are most likely caused by the different dimensions of the samples used in the two cases. However, dehydration at higher temperature and for longer time as described above is accompanied by a simultaneous decoloration of the sample, faster in the light zones and slower in the dark ones just in accordance with what was observed by Taran and Koch-Müller (2010). After final thermal annealing (at 1200 °C, 5 hours) the sample acquires a homogenous light greenish-yellow color, showing no sign of the intense $\mathbf{E}\parallel\mathbf{c}$ -polarized $\text{Fe}^{2+}/\text{Ti}^{4+}$ IVCT band at $\sim 20500 \text{ cm}^{-1}$ (Fig. 8). The spectra in $\mathbf{E}\parallel\mathbf{a}$ - and $\mathbf{E}\parallel\mathbf{b}$ -polarizations remain nearly the same as in the initial untreated sample.

Protonation of the annealed sample in a hydrothermal capsule at 0.5 kbar, 650 °C and f_{O_2} corresponding to the Ni/NiO buffer does not induce any noticeable change in color, as well as in the optical absorption and FTIR spectra.

Discussion

The sharp absorption lines at (in cm^{-1}) 3247, 3275, 3437, 3461, 3480, 3516, 3527, 3598 and 3654, with similar polarization properties as in the light zone of our sample, all strong in $\mathbf{E}\parallel\mathbf{a}$ - and $\mathbf{E}\parallel\mathbf{b}$ -polarizations, but very weak in $\mathbf{E}\parallel\mathbf{c}$ (Fig. 2), were observed in natural andalusites by Burt et al. (2007). Note, however, that comparing with our sample the lines displayed rather different intensity ratios that immediately implies that there exist more than one type of OH-groups in natural andalusites.

According to Burt et al. (2007) the corresponding O – H-vectors lay predominately in the **ab**-plane, since all absorption lines are strong in $\mathbf{E}\parallel\mathbf{a}$ - and $\mathbf{E}\parallel\mathbf{b}$ -polarization, but nearly zero in $\mathbf{E}\parallel\mathbf{c}$. Their theoretical analysis reveals that potential oxygens for protonation in andalusite, which satisfy the above polarization properties, $\mathbf{E}\parallel\mathbf{a} \approx \mathbf{E}\parallel\mathbf{b} \gg \mathbf{E}\parallel\mathbf{c}$, are the oxygens O1 and O2. Fig. 9 a,b show clusters around the O1 and O2 sites, respectively, projected on (001) of the andalusite structure including the proposed hydrogen sites (Burt et al. 2006, 2007). The O1 site is

coordinated by three Al atoms and the O2 site by two Al and one Si atom. The oxygen sites O1 and O2 were already discussed by Beran and Zemmann (1969) as possible hosts for hydrogen. Johnson (2006) suggested that hydrogen incorporates into andalusite (and also into kyanite and sillimanite) via the exchange mechanism $3\cdot\text{OH}^- + \text{vacancy} \leftrightarrow \text{Al}^{3+} + 3\text{O}^{2-}$. She did not consider that andalusite may contain other two-valent cations which can facilitate hydrogen incorporation through coupled substitutions, e.g. $\text{Fe}^{2+} + \text{H}^+ = \text{Al}^{3+}$ (e.g. Beran and Zemmann, 1969).

The composition of the andalusite of this study (see the Results section) is practically identical to that described previously by Taran and Koch-Müller (2010), i.e. it is rather a pure material admixed by only ~0.43 wt. % iron calculated as FeO and traces of titanium. As seen from the presence of the $\text{Fe}^{2+}/\text{Ti}^{4+}$ IVCT band and a weak ${}^5T_{2g} \rightarrow {}^5E_g$ spin-allowed band of ${}^VI\text{Fe}^{2+}$ (Fig. 1), some of the Fe is obviously ferrous iron and the structure must be partly charge compensated by a neighboring Ti^{4+} . Besides, the curve-fitting analysis resolves a weak $\mathbf{E}||\mathbf{c}$ -band at $\sim 14000\text{ cm}^{-1}$ assigned to $\text{Fe}^{2+}/\text{Fe}^{3+}$ IVCT transition (Taran and Koch-Müller 2010) that evidences of some amount of octahedral Fe^{2+} which is very likely charge balanced over the coupled $\text{Al}^{3+} \leftrightarrow \text{Fe}^{2+} + \text{H}^+$ substitution.

As concluded by Meisel et al., (1990) the Fe^{2+} content in andalusite is limited, e.g. by the presence of Ti^{4+} or "other cations providing the charge compensation". If we assume that beside of Ti^{4+} hydrogen is a charge compensating cation, we would need ~ 17 % of the Fe incorporated as Fe^{2+} . Mössbauer spectroscopic studies (Halenius 1978; Meisel et al. 1990) proved that Fe^{2+} does incorporate into the andalusite structure. Depending on the total iron concentration the $\text{Fe}^{3+}/\text{Fe}^{2+}$ ratio varies from 1.0 (0.3 wt% Fe; Meisel et al. 1990) for low iron concentrations to 13 for high iron concentrations (3 wt% Fe; Halenius 1978) leading to a Fe^{2+} concentration of 2000 to 5000 mole ppm. If we assume that all the hydrogen (1717 mole ppm H) in the andalusite under study are charge compensated by Fe^{2+} , we end up with a very low Fe^{2+} content (see above) and a $\text{Fe}^{3+}/\text{Fe}^{2+}$ ratio of 4.6 – closer to the value of Meisel et al. (1990) than to Halenius (1978). Therefore, in this particular case there is no need to introduce Al-vacancies for hydrogen intake:

it seems certain that hydrogen may incorporate into the actual andalusite structure not via the exchange mechanism $3\cdot\text{OH}^- + \text{vacancy} \leftrightarrow \text{Al}^{3+} + 3\text{O}^{2-}$, but mostly due to the coupled substitution $\text{Al}^{3+} \leftrightarrow \text{Fe}^{2+} + \text{H}^+$ for charge balancing.

The weakening and disappearance of the $\text{Fe}^{2+}/\text{Ti}^{4+}$ IVCT band in the andalusite spectra under annealing in air is caused by oxidization of Fe^{2+} to Fe^{3+} in IVCT $\text{Fe}^{2+}/\text{Ti}^{4+}$ pairs. The process of oxidation is accompanied by a rearrangement of the hydroxyl groups and dehydration of the sample, especially vivid at the final stage of the thermal annealing at 1200 °C (Figs. 4, 5). During thermal annealing structural hydroxyls of different types apparently transform to each other, the most distinct are the hydroxyls causing the doublet at 3516 cm^{-1} and 3527 cm^{-1} and those responsible for the characteristic lines at 3437 and 3480 cm^{-1} . They seem to transform into the hydroxyls causing the line at 3461 cm^{-1} . The line at 3461 cm^{-1} which is present in the spectra of the untreated sample and which increases at the expense of other OH bands during annealing (Figs. 4 -7), is to be related to Fe^{3+} . For charge balancing it seems reasonable to imply that the line is related to Fe^{3+} at a tetrahedral Si-site ($\text{Fe}^{3+} + \text{H}^+ \rightarrow \text{Si}^{4+}$). Since O1 and O2 are the most probable oxygen ions for protonation (Burt et al. 2007), we assume that the decrease of the doublet at 3516 cm^{-1} and 3527 cm^{-1} accompanied by the increase of the line at 3461 cm^{-1} (Figs. 4, 5), as well as a slight change of $\mathbf{E}||\mathbf{a}/\mathbf{E}||\mathbf{b}$ intensity ratio of the later (cf. Figs. 2 and 7), is just the direct evidence of a transformation of one type of OH-groups to another, namely, those, located on O1 to those on O2. Thus, we suggest the following scenario: vibrations of the O1-H1a,b dipoles (neighboring octahedral and five-fold coordinated Al-sites - one occupied by Fe^{2+} ; Fig. 9a), cause the strong doublet at 3516 cm^{-1} and 3527 cm^{-1} in the infrared spectra; vibrations of the O2 – H2a,b dipoles (neighboring 2 Al-sites and one tetrahedral Si-site occupied by Fe^{3+} ; Fig. 9b) cause the line at 3461 cm^{-1} . During annealing, Fe^{2+} at the octahedral sites oxidizes to Fe^{3+} and H is deliberated for charge balancing (decrease of the corresponding OH band and the IVCT band) while the amount of Fe^{3+} plus H at the tetrahedral Si-sites increases (increase of the corresponding OH band). This process must be accompanied by an increase of Fe^{3+} and decrease

of Si at the Si-site - most probably due to thermally induced diffusion. All spectral observations during heating can be explained with such a process.

The fact that we failed to restore, even partly, the red color (as well as $\text{Fe}^{2+}/\text{Ti}^{4+}$ IVCT band in the andalusite spectrum) and even to a minor extent increase the intensity of the OH-absorption lines in the protonation experiment (see Results) evidences, most probably, that thermally induced cationic diffusion during annealing to 1200 °C leads to dispersion of Fe and Ti, combined in the initial natural sample into $\text{Fe}^{2+}\text{-Ti}^{4+}$ and $\text{Fe}^{2+}\text{-Fe}^{3+}$ IVCT pairs, among the structural sites after or together with Fe^{2+} to Fe^{3+} oxidation. This leads to the subsequent reduction $\text{Fe}^{3+} \rightarrow \text{Fe}^{2+}$ and "recovery" of the IVCT pairs in the protonation experiment at 650 °C.

Comparison of the spectra of the zoned crystal studied here (Figs. 2, 3) and their thermal evolution (Figs. 4-7) obviously evidences that there are several types of OH-groups in the andalusite structure, all having hydrogen located in the (001) plane. In the initial, untreated state, we can distinguish at least two different types of hydroxyls in the light and dark zones of the sample as follows from different polarization properties of the absorption lines at 3437 and 3480 cm^{-1} (see Results). As for us, the most interesting aspect of this study is that there is a strict relation between the red to black color of andalusite, caused by electronic $\text{Fe}^{2+}/\text{Ti}^{4+}$ IVCT transition between Fe^{2+} and Ti^{4+} in the adjacent octahedral sites, and some part of hydroxyls in the andalusite structure. The presence or absence of the $\mathbf{E}\parallel\mathbf{b}$ -polarized components of the two absorption lines at 3480 cm^{-1} and 3437 cm^{-1} can only be interpreted (e.g. Libowitzky and Rossmann 1996) that hydroxyls of a certain type, which cause these lines, are differently oriented in the two zones, light and dark. And, as far as we are aware, this is the first observation of such kind of OH-reorientation in a mineral structure. The same holds for the change of the polarization behavior of the 3461 cm^{-1} band in the dark and light zone during annealing. After annealing at 1200°C the intensity of the band measured with $\mathbf{E}\parallel\mathbf{a}$ is significantly higher in the spectra of the dark zone than in the spectra of the light zone, where the $\mathbf{E}\parallel\mathbf{b}$ bands dominates. Thus, there must be a rearrangement of the OH vectors in the dark zone compared to the light

one caused by annealing. As found out by Taran and Koch-Müller (2010) the compositions of the light and dark zone in andalusites studied differ slightly in the concentration of iron and titanium impurities, either isolated or combined into pairs or some more complicate aggregates in adjacent octahedral sites elongated parallel to the **c**-axis of the structure. A part of Fe and Ti is involved into electronic $\text{Fe}^{2+}/\text{Ti}^{4+}$ IVCT transition which causes the broad intense $\mathbf{E}\parallel\mathbf{c}$ -polarized optical absorption band at $\sim 20500\text{ cm}^{-1}$ and red coloration of the crystals in this polarization. Now, it looks quite certain that at least a part of hydroxyl groups is tightly related in some way to the admixture of iron and titanium. It seems also certain that in the dark zones, enriched with Fe and Ti, some portion of OH groups, causing the absorption lines at 3480 cm^{-1} and 3437 cm^{-1} , both strictly $\mathbf{E}\parallel\mathbf{a}$ -polarized, should interact in some way with $\text{Fe}^{2+}\text{-Ti}^{4+}$ -pairs or some other combinations of these ions. By the interaction their O – H-vector aligns parallel to **a**-axis thus causing zero intensity of the absorption lines in question at $\mathbf{E}\parallel\mathbf{b}$ and $\mathbf{E}\parallel\mathbf{c}$ (Figs. 2b, 3b). The mechanism of such reorientation is not quite clear, but it is most probably caused by a redistribution of the electronic density along the bond between Fe^{2+} and Ti^{4+} ions in IVCT pairs or complexes. Note that the concentration of $\text{Fe}^{2+}/\text{Ti}^{4+}$ IVCT pairs in the dark zones are estimated to be nearly four times higher than in the light ones (Taran and Koch-Müller 2010). Fig. 10 shows a fragment of the andalusite structure with four adjacent elongated octahedral AlO_6 sites, which may be occupied by Fe^{2+} and Ti^{4+} . In addition two possible OH-groups bonded to O1 as suggested by Burt et al. (2007) are shown. We aligned one OH vector strictly parallel to the **a**-axis – it could represent the OH vector responsible for the OH bands of the dark zone and the other one laying in the **ab**-plane could represent the OH vector of the light zone. Similar rearrangement could be the cause of the change in polarization behavior of the 3461 cm^{-1} band in the light and dark zone.

We observed that the rate of bleaching depends on sample geometry and sample thickness. This is in a good accord with observation that the diffusion rates measured on single crystals are often much slower than those measured using bulk experiments on powdered

materials (Farver 2010). Judging from the information on hydrogen uptake/extraction in minerals (Ingrin and Blanchard 2006), the process of hydrogen uptake may be accompanied by iron reduction from Fe^{3+} to Fe^{2+} . This suggests that hydrogen extraction in andalusite can also be controlled by redox reactions, which, as we assume on the basis of optical absorption spectroscopy studies (Taran and Koch-Müller 2010), leads to the discoloration of the sample due to $\text{Fe}^{2+} \rightarrow \text{Fe}^{3+}$ oxidation in $\text{Fe}^{2+}\text{-Ti}^{4+}$ pairs and aggregates. Cationic diffusion at temperatures up to 1200 °C may also play a significant role in irreversible thermal destruction of $\text{Fe}^{2+}/\text{Ti}^{4+}$ and $\text{Fe}^{2+}/\text{Fe}^{3+}$ IVCT pairs preventing their recovery at protonation experiments.

Acknowledgments

Stanislav Matsyuk, Kiev, helped with the oriented sample preparation. Alexej Vishnevskyy, Kiev, made up the microprobe analysis of the sample. Two official reviewers, Ulf Hålenius, Stockholm, and an anonymous reviewer gave a lot of very helpful comments and suggestions that significantly improved the paper. The German Science Foundation, Bonn-Bad Godesberg, generously supported this work through traveling grant KO1260/13-1. We are grateful to these individuals and institution for their help.

References

- Bell DB, Rossman GR, Maldener J, Endisch D, Rauch F (2004) Hydroxide in kyanite: a quantitative determination of the absolute amount and calibration of the IR spectrum. *Am Mineral* 89: 998 – 1003
- Beran A, Zemann J (1969) Messung des Ultrarot-Pleochroismus von Mineralen VIII. Der Pleochroismus der OH-Streckfrequenz in Andalusit. *Tsch Miner Petro Mitt* 13: 285 - 292
- Burt JB, Ross NL, Ross JA, Koch M (2006) Equations of state and structures of andalusite to 9.8 GPa and sillimanite to 8.5 GPa. *Am Mineral* 91: 319 - 326
- Burt JB, Ross NL, Gibbs GV, Rossman GR, Rosso KM (2007) Potential protonation sites in the Al_2SiO_5 polymorphs based on polarized FTIR spectroscopy and properties of the electron density distribution. *Phys Chem Minerals* 34: 295–306
- Farver JR (2010) Oxygen and Hydrogen Diffusion in Minerals. *Reviews in Mineralogy and Geochemistry* 72: 447-507
- Halenius U (1978) A spectroscopic investigation of mangian andalusite. *Can Mineral* 16: 567-575
- Johnson EA (2006) Water in Nominally Anhydrous Crustal Minerals: Speciation, Concentration, and Geologic Significance. *Reviews in Mineralogy and Geochemistry* 62: 117-154
- Ingrin J, Blanchard M (2006) Diffusion of hydrogen in minerals. *Reviews in Mineralogy and Geochemistry* 62: 291-320
- Koch-Müller M, Rhede D (2010) IR absorption coefficients for water in nominally anhydrous high-pressure minerals. *Am Mineral* 93: 770 - 775
- Libowitzky E, Rossman GR (1997) An IR absorption calibration for water in minerals. *Am Mineral* 82: 1111–1115

- Meisel W, Schnellrath J, Griesbach P, Gutlich P (1990) The state of iron in andalusite. *Hyperfine Interactions* 57: 2261-2268
- Rossmann GR (1996) Studies of OH in nominally anhydrous minerals. *Phys Chem Minerals* 23: 299-304
- Smith G (1977) Low-temperature optical studies of metal-metal charge-transfer transitions in various minerals. *Canad Mineral* 15: 500-507
- Smith G, Strens RGJ (1976) Intervalence transfer absorption in some silicate, oxide and phosphate minerals. In: Strens RGJ (ed) *The Physics and Chemistry of Minerals and Rocks*. Wiley, New York, 583-612
- Taran MN, Koch-Müller M (2011) Optical absorption of electronic Fe–Ti charge-transfer transition in natural andalusite: the thermal stability of the charge-transfer band. *Phys Chem Minerals* 38: 215–222

Captions for Figures

Fig. 1. $\mathbf{E}\parallel\mathbf{c}$ -polarized optical absorption spectra of the two differently colored zones of the andalusite sample studied, light and dark.

Fig. 2. Polarized FTIR spectra, measured in two differently colored zones, light (a) and dark (b), of the Brazilian andalusite studied. The spectra were recalculated for the sample thickness 1 cm.

Fig. 3. Result of 20 steps scanning of $\mathbf{E}\parallel\mathbf{b}$ -polarized spectra across differently colored zones of the andalusite sample studied (a) and an image of the \mathbf{bc} -plane of the sample at transmitting $\mathbf{E}\parallel\mathbf{c}$ -polarized illumination (b). The white line indicates the path of the scanning from right down to left up.

Fig. 4. Evolution of $\mathbf{E}\parallel\mathbf{b}$ -polarized spectrum of the light zone at annealing at different temperatures and durations in air: 1- initial natural sample; 2 – 800 °C, 2 hours, 3 - 900 °C, 2 h; 4 - 1000 °C, 2 h; 5 - 1000 °C, 4 h; 6 - 1000 °C, 8 h; 6 - 1000 °C, 13 h; 7 - 1100 °C, 4 h; 8 - 1200 °C, 5 h.

Fig. 5. Evolution of $\mathbf{E}\parallel\mathbf{a}$ -polarized spectrum of the light zone at annealing at different temperatures and durations in air: 1- initial natural sample; 2 – 500 °C, 2 hours, 3 - 700 °C, 2 h; 4 - 900 °C, 2 h; 5 - 1000 °C, 2 h; 6 - 1000 °C, 8 h; 7 - 1000 °C, 13 h; 8 - 1200 °C, 5 h.

Fig. 6. FTIR spectra of the light (a) and dark zone (b) after thermal annealing at 1100 °C during 10 hours.

Fig. 7. Polarized FTIR spectra of the two differently colored zones, light (a) and dark (b), in the andalusite sample studied after the final stage of annealing at 1200 °C during five hours.

Fig. 8. Polarized optical absorption spectra of the andalusite sample studied after its final annealing at 1200 °C during five hours.

Fig. 9 Projection of clusters of the andalusite structure around the O1 site (a) and O2 site (b) based on structural data of Burt et al. (2006) with the hydrogens arranged as suggested by

Burt et al. (2007). Vibrations of the O1-H1 dipoles (neighboring octahedral and five-fold coordinated Al-sites - one occupied by Fe^{2+}) are assigned to cause the strong doublet at 3516 cm^{-1} and 3527 cm^{-1} in the infrared spectra and vibrations of the O2 – H2 dipoles (neighboring 2 Al-sites and one tetrahedral Si-site occupied by Fe^{3+}) are assigned to cause the line at 3461 cm^{-1} . During annealing, Fe^{2+} at the octahedral sites oxidizes to Fe^{3+} and H is deliberated for charge balancing (decrease of the corresponding OH band and the IVCT band) while the amount of Fe^{3+} plus H at the tetrahedral Si-sites increases (increase of the corresponding OH band).

Fig. 10. A fragment of the andalusite structure with four adjacent elongated along **c**-axis octahedral AlO_6 -sites which may be occupied by Fe^{2+} and Ti^{4+} . Two possible positions of protons on O1 are conditionally shown: that with OH-vector laying in the **ab**-plane (the light zone case), and that with OH-vector strictly parallel **a**-axis (the dark zone case).

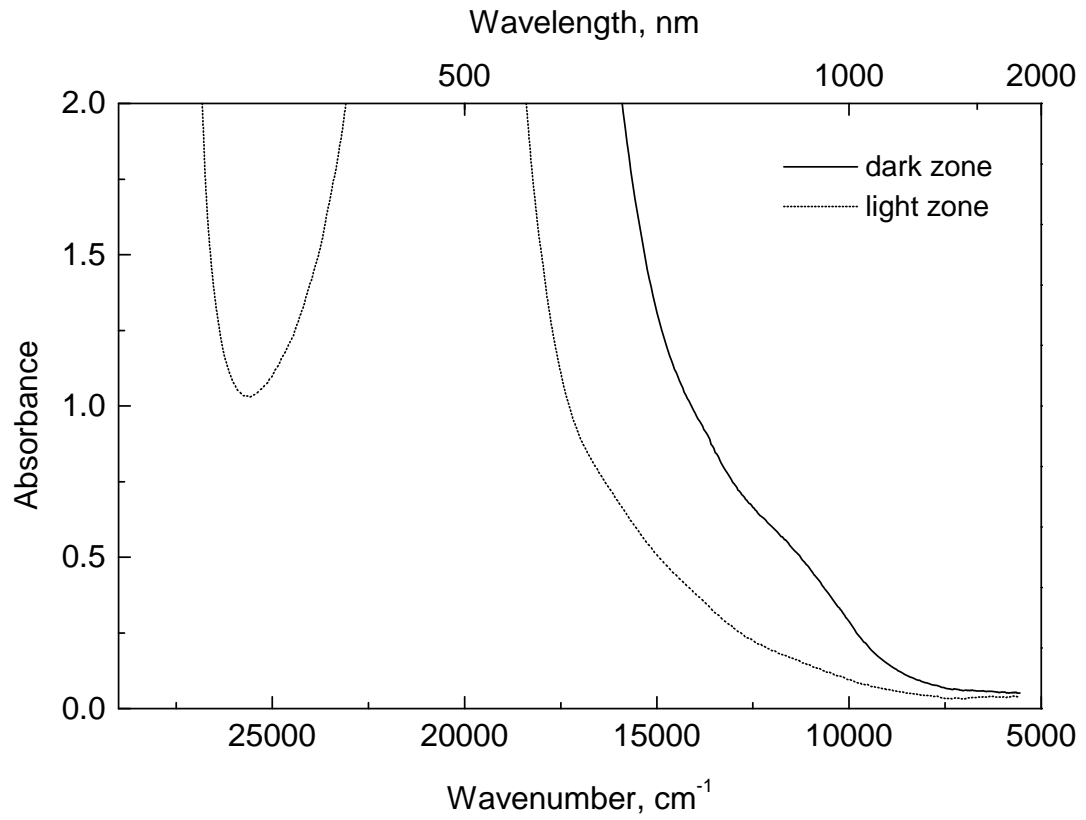


Fig. 1. $\mathbf{E}||\mathbf{c}$ -polarized optical absorption spectra of the two differently colored zones of the andalusite sample studied, light and dark.

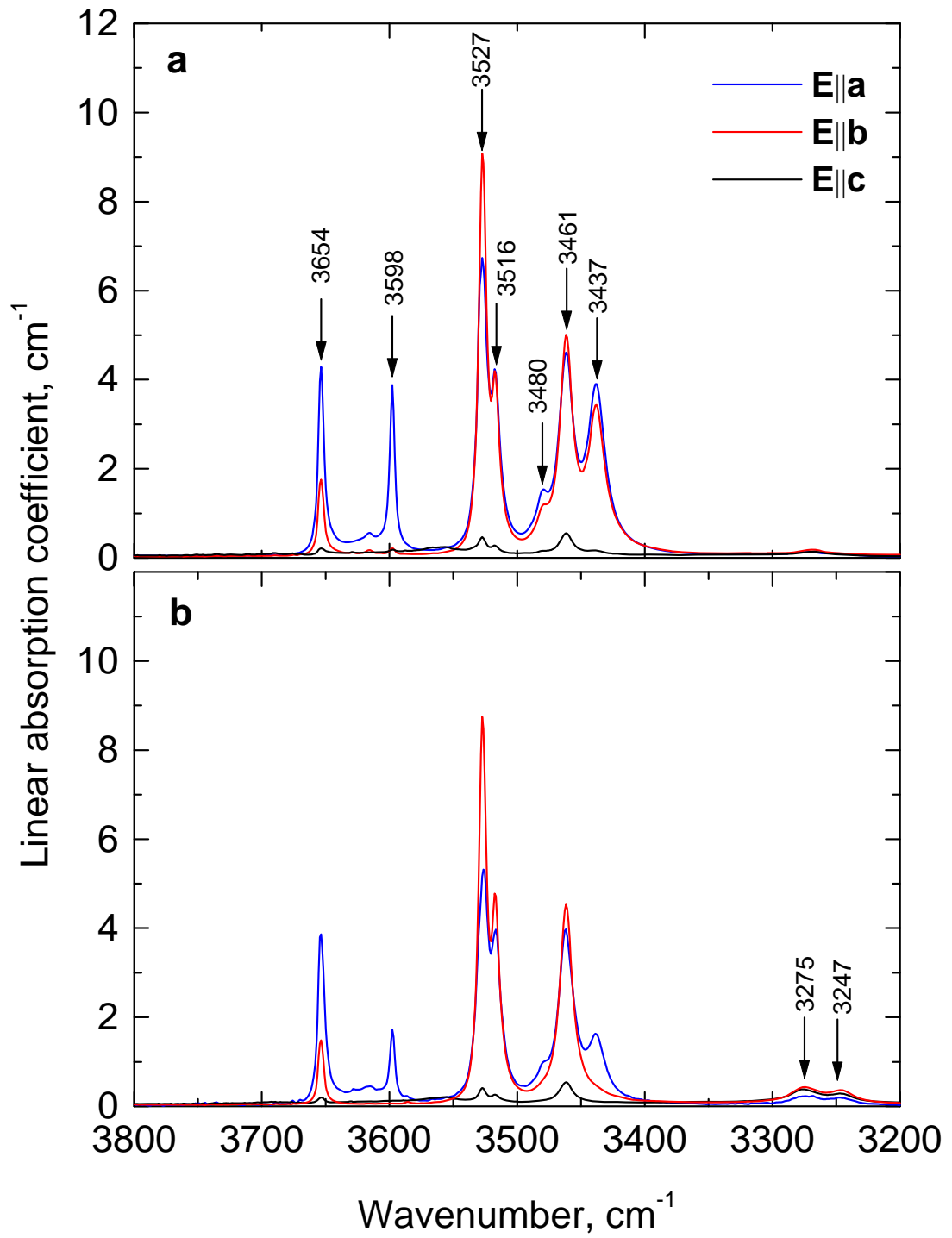


Fig. 2. Polarized FTIR spectra of the Brazilian andalusite studied, measured in two differently colored zones, light (a) and dark (b).

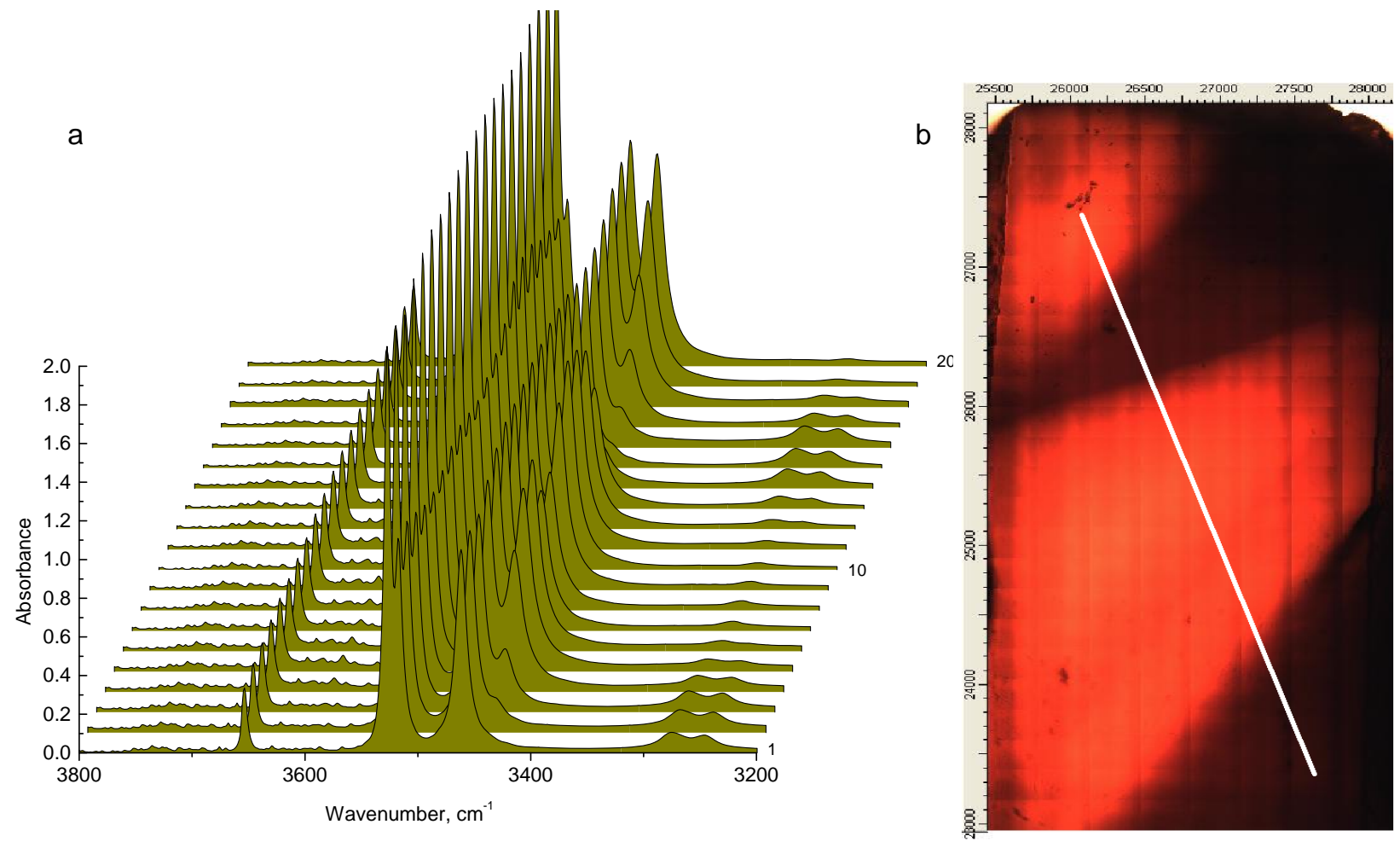


Fig. 3. Result of 20 steps scanning of $\mathbf{E}||\mathbf{b}$ -polarized spectra across differently colored zones of the andalusite sample studied (a) and an image of the \mathbf{bc} -plane of the sample at transmitting $\mathbf{E}||\mathbf{c}$ -polarized illumination. The white line indicates the path of the scanning from right down to left up (b).

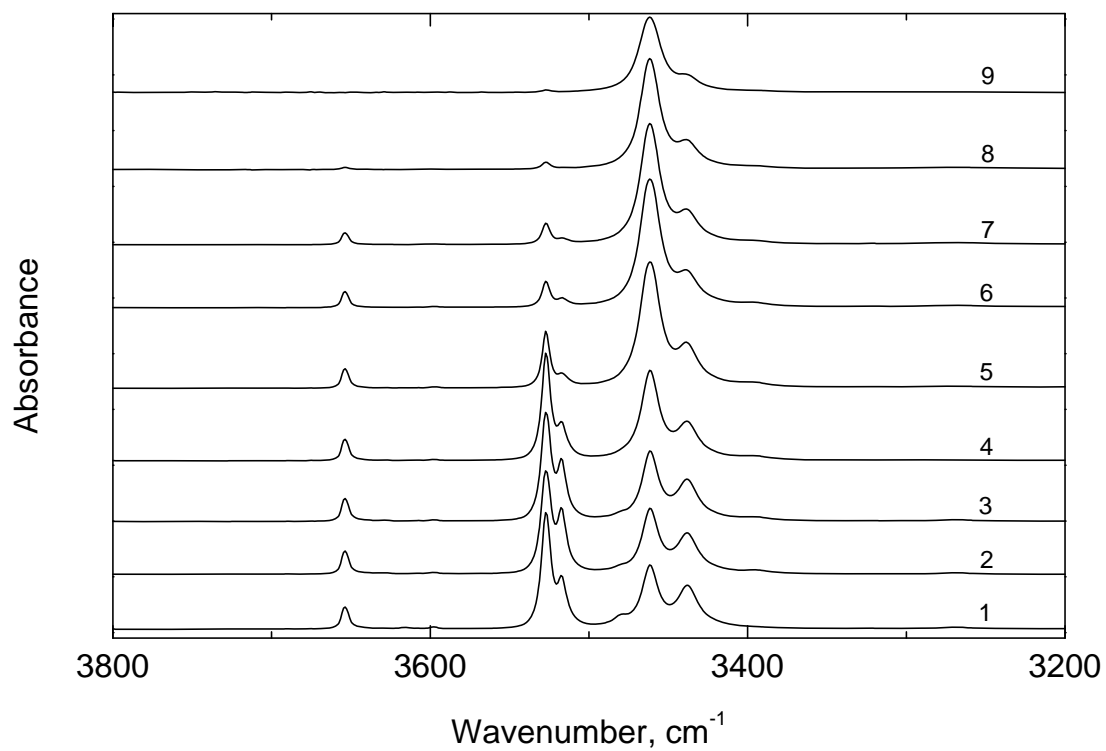


Fig. 4. Evolution of $E||b$ -polarized spectrum of the light zone at annealing at different temperatures and durations in air: 1- initial natural sample; 2 – 800 °C, 2 hours, 3 - 900 °C, 2 h; 4 - 1000 °C, 2 h; 5 - 1000 °C, 4 h; 6 - 1000 °C, 8 h; 6 - 1000 °C, 13 h; 7 - 1100 °C, 4 h; 8 - 1100 °C, 10 h; 9 - 1200 °C, 5 h.

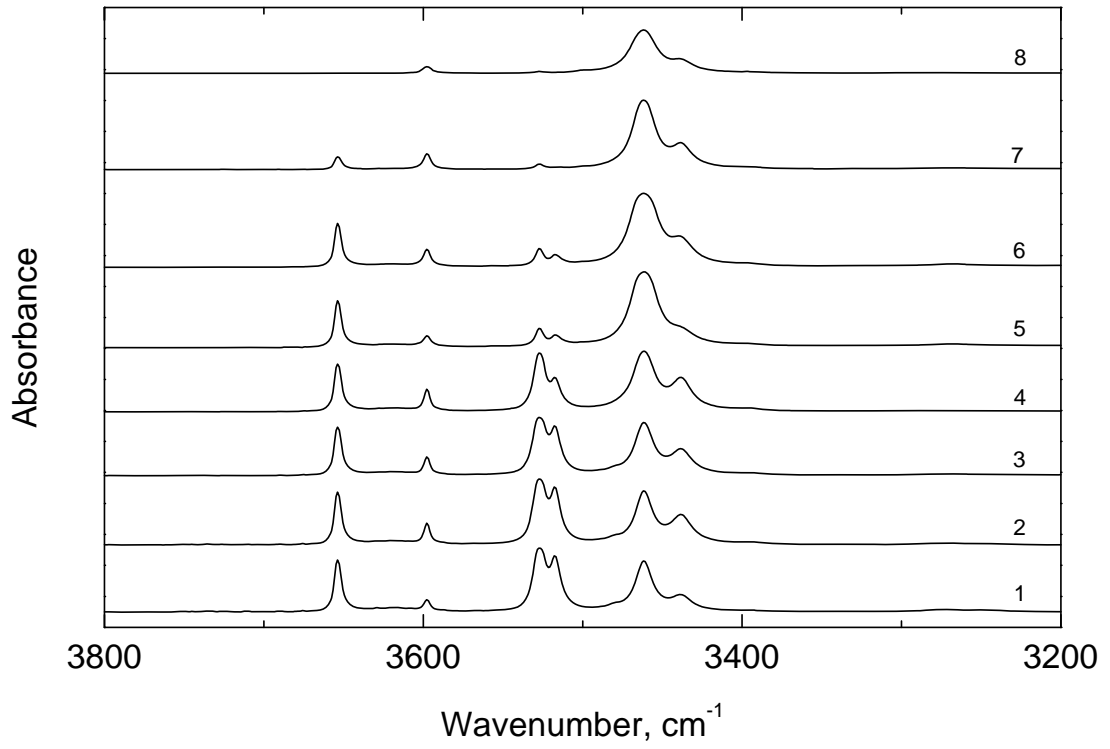


Fig. 5. Evolution of $E||a$ -polarized spectrum of the light zone at annealing at different temperatures and durations in air: 1- initial natural sample; 2 – 500 °C, 2 hours, 3 - 700 °C, 2 h; 4 - 900 °C, 2 h; 5 - 1000 °C, 2 h; 6 - 1000 °C, 8 h; 7 - 1000 °C, 13 h; 8 - 1200 °C, 5 h.

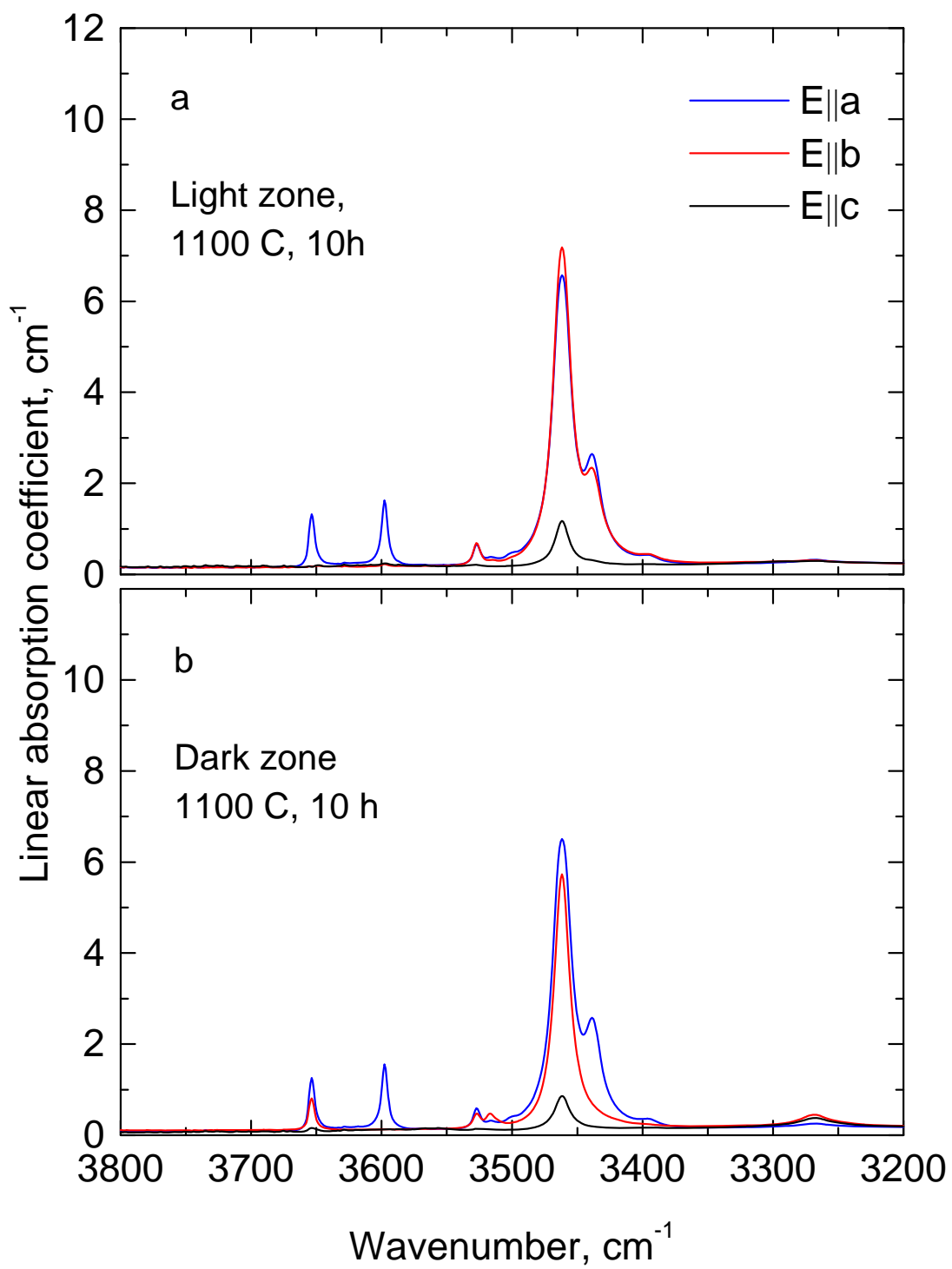


Fig. 6. FTIR spectra of the light (a) and dark zone (b) after thermal annealing at 1100 °C during 10 hours.

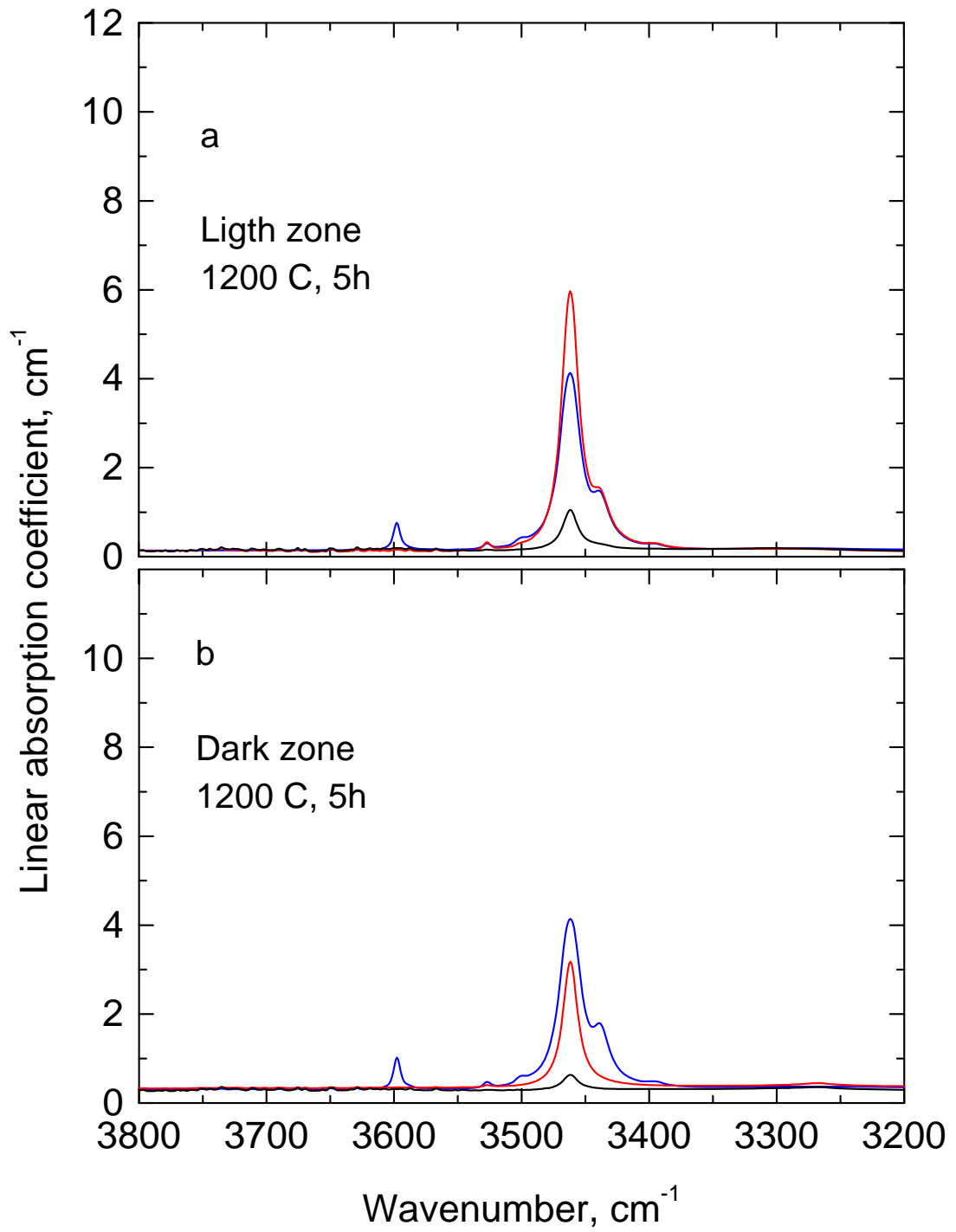


Fig. 7. Polarized FTIR spectra of the two differently colored zones, light (a) and dark (b), in the andalusite sample studied after the final stage of annealing at 1200 °C during five hours.

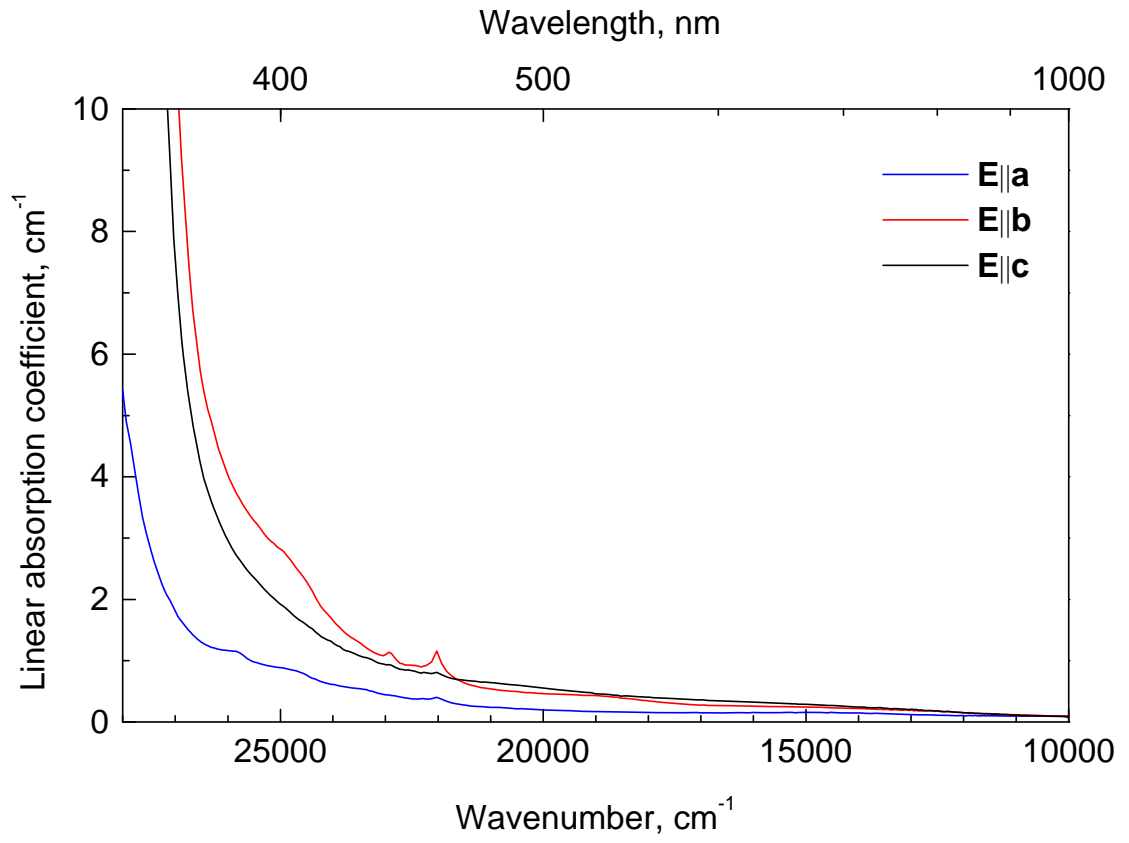


Fig. 8. Polarized optical absorption spectra of the andalusite sample studied after its final annealing at 1200 °C during five hours.

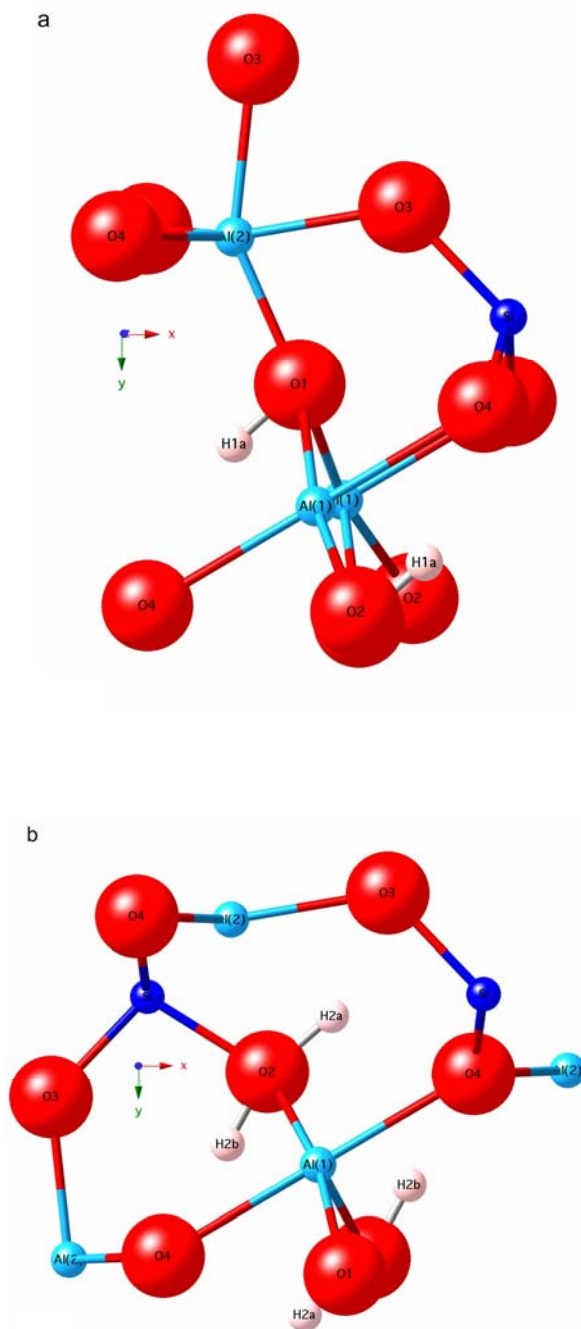


Fig. 9. Projection of clusters of the andalusite structure around the O1 site (a) and O2 site (b) based on structural data of Burt et al. (2006) with the hydrogens arranged as suggested by Burt et al. (2007). Vibrations of the O1-H1 dipoles (neighboring octahedral and five-fold coordinated Al-sites - one occupied by Fe^{2+}) are assigned to cause the strong doublet at 3516 cm^{-1} and 3527 cm^{-1} in the infrared spectra and vibrations of the O2 – H2 dipoles (neighboring 2 Al-sites and one tetrahedral Si-site occupied by Fe^{3+}) are assigned to cause the line at 3461 cm^{-1} . During annealing, Fe^{2+} at the octahedral sites oxidizes to Fe^{3+} and H is deliberated for charge balancing (decrease of the corresponding OH band and the IVCT band) while the amount of Fe^{3+} plus H at the tetrahedral Si-sites increases (increase of the corresponding OH band).

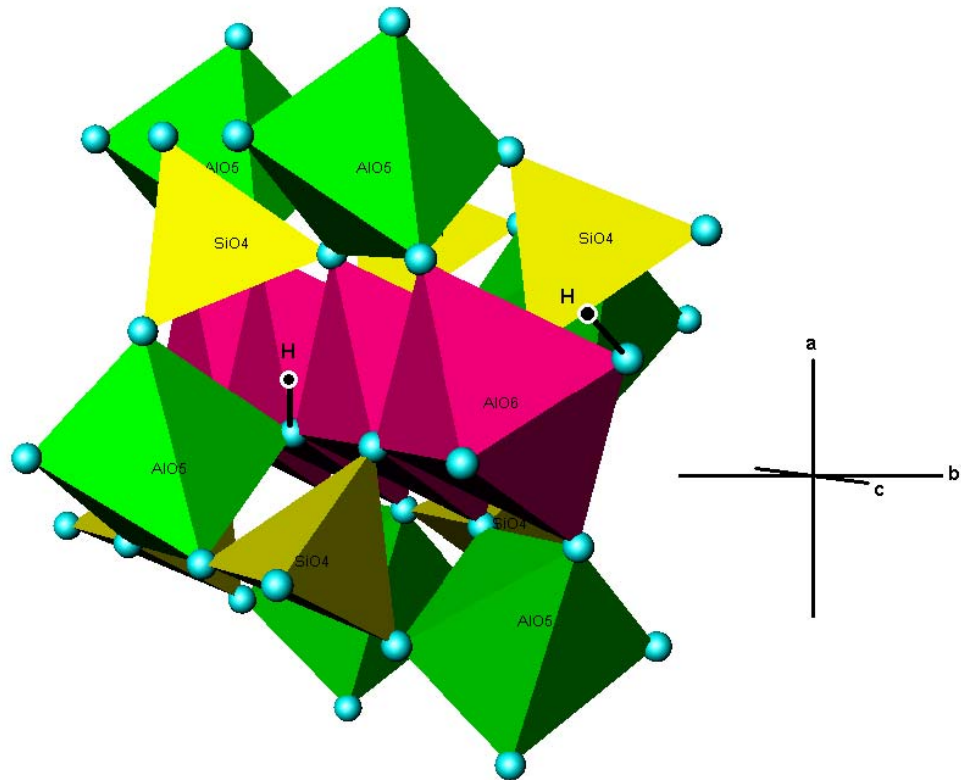


Fig. 9. A fragment of the andalusite structure with four adjacent elongated along **c**-axis octahedral AlO_6 -sites which may be occupied by Fe^{2+} and Ti^{4+} . Two possible positions of protons on O1 are conditionally shown: that with OH-vector laying in the **ab**-plane (the light zone case), and that with OH-vector strictly parallel **a**-axis (the dark zone case).